Periodica Polytechnica
Civil Engineering

60(3), pp. 437–448, 2016
DOI: 10.3311/PPci.8661

RESEARCH ARTICLE

Modelling Methods Attached to the Research of Groundwater Flow in Fractured Rocks – Theories, Laboratory and Numerical Modelling

Gyöngyi Karay, *Géza* Hajnal
Received 09-10-2015, revised 12-01-2016, accepted 14-01-2016

Abstract

There are serious efforts worldwide to better understand and model groundwater flow in fractured rocks and karst aquifers. This study summarizes the major theories and idealizations used for describe flow in fractured rocks and presents a laboratory model and numerical models which were made for this purpose. The laboratory model originally made by Öllős and Németh in 1960 was rebuilt in MODFLOW-CFP. The usability of both modelling method was analysed. Based on the experience of this modelling an existing cave system was modelled with CFP. The Molnár János Cave – a karst cave almost filled with water – was analysed with the tool of numerical modelling to better understand the flow in cave conduits.

Keywords

fractured rocks · karst · laboratory model · MODFLOW-CFP · Molnár János Cave

Gyöngyi Karay

Department of Hydraulic and Water Resources Engineering, Faculty of Civil Engineering, Budapest University of Technology and Economics, Műegyetem rkp. 3, H-1111 Budapest, Hungary
e-mail: karay.gyongyi@epito.bme.hu

Géza Hajnal

Department of Hydraulic and Water Resources Engineering, Faculty of Civil Engineering, Budapest University of Technology and Economics, Műegyetem rkp. 3, H-1111 Budapest, Hungary
e-mail: hajnal.geza@epito.bme.hu

1 Introduction

The importance of the research of the water flow in fractured rocks is obvious: many Hungarian and worldwide examples demonstrate its role in water supply (e.g. Bükk Karst Aquifer in Hungary, Brestovica Karst Aquifer in Slovenia [1], Haute-Normandie Region in France [2], Bernese Jura in Switzerland [3], Madison Aquifer in the United States [4], Yucatán Karst in Mexico [5] etc.), but it also can influence mining and civil engineering works, cannot be forgotten when constructing nuclear waste repositories (Bátaapáti in Hungary and many examples from Europe and America in [6]), furthermore, their recreation role also could be serious. Moreover, many fields of life, economy and science can be interested in research of karst and fractured rock aquifers but there are some difficulties which differ from the traditional groundwater problems. The often assumed homogeneity and isotropy of the media in which the groundwater flows is not valid in case of water flow in fractured rocks. Moreover, Darcy's law is usable only if the flow is slow and laminar and the pores are small. The flow in porous media usually fulfils these criteria but in fractured rocks the water flow could be quite fast and non-laminar and there are orders of magnitude differences between the sizes of discontinuities. These led to the development of special modelling theories and methods which take into account the characteristics of flow in fractured rocks.

1.1 The double porosity theory

One of the most evident differences between porous and fractured media is the high variance in sizes of discontinuities. Next to the pores which can be observed also among the particles of porous media and in the intact fractured rocks – this is the so called matrix porosity – more discontinuities as fractures, voids and karst conduits can exist in fractured rocks. Against the matrix porosity which has the same age like the media the fractures are mostly formed later by tectonic movement or other forces. Barenblatt et al. introduced the double porosity theory which handles these additional discontinuities as secondary porosity next to the matrix porosity named primary porosity [7]. The two types of porosity have different properties: flow in the primary porosity is slow, the hydraulic conductivity is low and

the storativity is quite high; but in secondary porosity the water flow might be fast and non-laminar, the hydraulic conductivity is significant higher but the storativity is lower than in the matrix porosity. The double-porosity theory was extended with the definition of tertiary porosity; the fractures originally belonging to the secondary porosity were enlarged by solution processes; these conduits with enlarged size and permeability occur in carbonate sedimentary rocks which are prone to karstifications. Traditional methods and software can solve groundwater flow in primary porosity but these could lead to wrong results where the role of the secondary porosity is predominant. Therefore, new methods are needed to improve the calculations of flow in dual porosity rocks.

1.2 Modelling approaches of flow in fractured rocks

The inhomogeneity and anisotropy of the fractured rocks make groundwater flow modelling more difficult than flow modelling in porous media although both phenomena can occur in analysis of porous rocks (for example [8–10]). It is essential to decide before modelling which parts of the system and which processes are relevant; the chosen method of idealisation forecasts the expected results. Because of its complexity there are more idealisation methods to describe the fractured media as accurately as it is necessary.

The modelling methods have two major approaches: continuum models and discrete models.

The continuum models partly ignore the geometry of the fractures and conduits. Their effects on flow are taken into account by parameter distribution along the entire continuum. In the continuum modelling the major effort is directed to define the representative elementary volume (REV), the minimum volume of the media which keeps the features of the entire volume. The simplest and easiest continuum model is the single continuum model or equivalent porous media approach. The groundwater flow is calculated with Darcy's law as it would be in case of an originally porous media; this idealisation allows the use of the common software of groundwater flow modelling (MODFLOW, FEFLOW etc.). The fractures and conduits are replaced with high permeable cells or layers. This method needs the fewest input parameters, and gives good water balance results but its application is limited because of the assumption of laminar flow. Examples for use of equivalent porosity models are: [11–13].

The double continuum model links the two flow regimes – one regime represents the rock matrix, the other regime represents the discontinuities – with an exchange term. The first regime is the so called diffuse flow regime which has low permeability and high porosity and the second is the higher velocity flow in conduits or fractures with lower porosity and higher permeability. Examples for its usage: [14, 15].

The discrete models require special discrete element modelling software (e.g. FLAC 3D) which is able to model the proper conduit/fracture geometry. This method needs the detailed knowledge of fracture network geometry and higher computing capacity than the continuum models. In the case when enough information about the geometry is not available fractures and conduits are often stochastically simulated [16, 17] or specified arbitrarily [18].

The so called hybrid models where the discrete discontinuity network is embedded in a continuum model provide more realistic idealisations of nature with the integrated treatment of slow groundwater flow in the rock matrix and fast flow in discontinuities even if the flow is non-laminar. The two flow regimes are also linked with the exchange term. The hybrid models can lead to more accurate spring discharges specially the peak discharges and more realistic flow pattern [19, 20]. Some of the widely used programs are now able to handle hybrid models: in FEFLOW a fracture network can be added as "Discrete features" [21], in MODFLOW the Conduit Flow Process was developed. More examples for usage of hybrid models: [22–24].

To model the discrete discontinuity network there are two current methods [25, 26]: fractures can be approached by planes [27, 28] or pipes [29–31]. Although the planes correspond better to the geometry of fractures, the assumption that water flows on the entire plane contradicts field experiments which showed that less than 10% of the fracture volume is used for water flow [32]. This so called channelling phenomenon – the water flows in tortuous paths on the plane – and the quite tubular karst conduits could be better approached by pipes. However, the model with tubes imbedded in the fracture planes assumes constant wall permeability and aperture along a tube which should also be a rough approximation.

1.3 Modelling techniques

In the previous point there were some numerical softwares mentioned which are able to calculate groundwater flow in fractured rocks under different assumptions. In this study the MODFLOW-CFP is used to hybrid modelling (about MODFLOW-CFP see [33]). On the other hand laboratory analog models were widely used before the spreading of the computer supported numerical modelling and these models nowadays have also a very important role also in helping to the understand the processes and verify numerical models.

In spite of their importance there are only few available studies about laboratory analog models of groundwater flow in fractured rocks. In Hungary well-known laboratory model researches were made by Géza Öllős and Endre Németh in the 1960s [34, 35]. Due to the development of numerical modelling methods the laboratory analog models had a minor roles in modelling of fractured rocks, but nowadays laboratory modelling is rediscovered. For example, laboratory models were made by Faulkner et al. in 2009 [36] and Wu and Hunkeler in 2013 [37].

2 Modelling in laboratory-scale

2.1 The laboratory model

The laboratory analog model made by Öllős and Németh [34] was an orthogonal grid which was built up by 0.6 m length PVC-

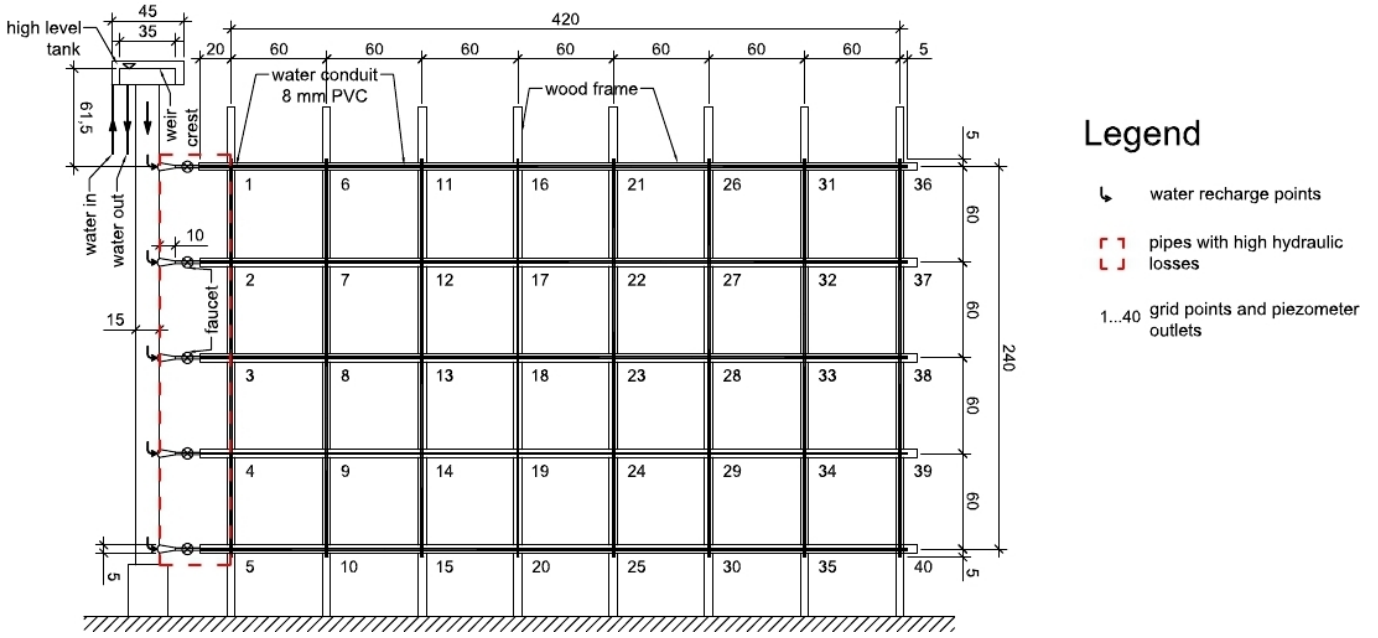

Fig. 1. The Öllős-Németh's laboratory model

pipes with 4.2 x 2.4 m overall size. The diameters of conduits were 8 mm. Constant water level was ensured on the left side of the model by a weir crest and at the end of the pipes were variable discharge points. More than 30 model cases were analysed by changing discharge points and model geometry. Hydraulic head data were collected in every grid points. For more details of the laboratory model see Fig. 1.

Based on this model a two dimensional MODFLOW CFP model was created.

2.2 Numerical model in CFP

For numerical simulation the laboratory analog model was rebuilt in MODFLOW-CFPv2 (CFP) using Mode 1 [38]. The model consists of 77 pipes and 46 nodes, 6 layers, 9 columns and 1 row. The water temperature was 15°C, the lower critical Reynolds number was 1000 and the upper was 2320. The constant head boundary on the left side of the model was 3.015 m. The different discharge points were modelled as "well" boundary conditions and the discharge rate was fixed according to the laboratory model. The geometry was slightly modified because the proper geometry with the intermediate faucets and confusors could not be modelled, but it became clear after some trial version that the effect of these faucets could not be ignored: the laboratory model results showed very high hydraulic losses between the high level tank and the first column of measuring points. This effect was modelled by decreasing the diameters in this initial section (see the pipes surrounded by dashed lines in Fig. 1). Originally the wall roughness of pipes was 1.5×10^{-6} m but with this value the hydraulic losses were lower in the numerical model than in the laboratory analog. Therefore, the initial diameter and the wall roughness were the calibrated parameters. The effects of these values did not relate to each other: the modification of the initial diameter changed the hydraulic losses between the high level tank and the first column of grid points; the roughness influenced the hydraulic head losses along the pipe grid. The time unit was *min* and the length unit was *cm* according to the units used in the laboratory model. For simplicity the hydraulic head data and discharges are given in these units.

The basis of the calibration was case A (see Table 1) with 5220 cm^3/min (8.7×10^{-5} m^3/s) discharge rate in the 38^{th} grid point. After the calibration there was good agreement between the laboratory and numerical model: the difference between measured and calculated hydraulic heads was under 1.5 cm except in the discharge point and in the nodes surrounding the discharge point. The equipotential lines of the laboratory and numerical models were quite parallel. The final value of wall roughness was 10^{-4} m and the initial diameter was 6.5×10^{-3} m.

The calibration results can be seen on Fig. 2.

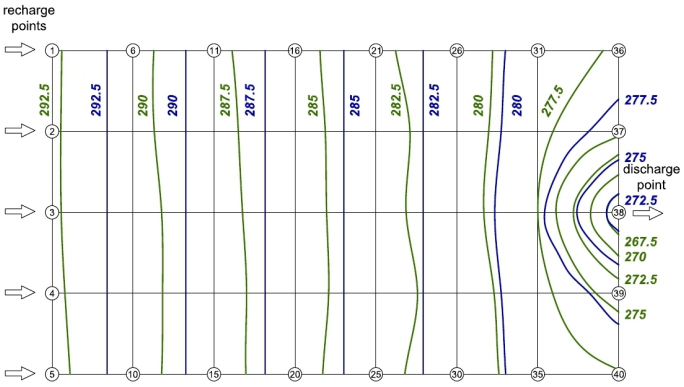

Fig. 2. Calibration results, model case A. Green/brighter lines: laboratory model results, blue/darker lines: numerical model results. Labels show potential in cm.

2.3 Model validation

After the calibration several other cases were analysed (see Table 1). Almost all numerical results were in correspondence

Tab. 1. Model cases in laboratory model

Model case identifier	Discharge point	Discharge rate (cm^3/min)	Other modifications	Head differences *(cm)*
A	38	5220		1.5 - 6
B	38	8400		5 - 9
C	40	4500		3 - 9
D	30	9000		9 - 11
E	20	4570	recharge points: 1,2	10.5 - 17
F	20, 38	4000, 4300	2 discharge points	4 - 8
G	30	8460	finer grid	2 - 9
H	20	8760	finer grid+6 thicker pipes	2.5 - 8 (2 - 7)
I	38	10080	finer grid+11 thicker pipes	10 - 19 (13 - 20)
J	20	9000	finer grid+11 thicker pipes	2.5 - 14 (5 - 12.5)

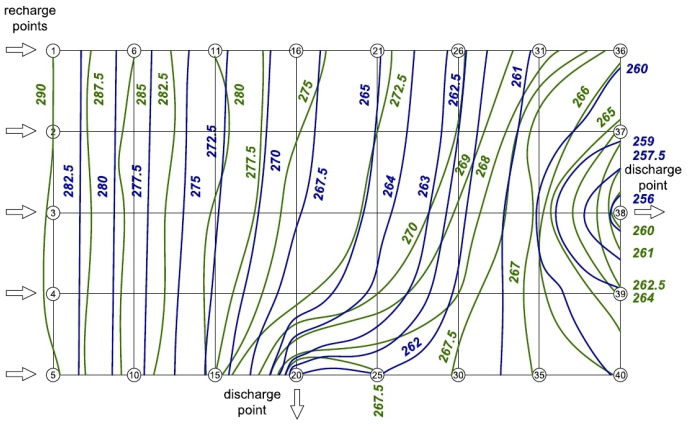

Fig. 3. Model case F. Green/brighter lines: laboratory model results, blue/darker lines: numerical model results. Labels show potential in cm.

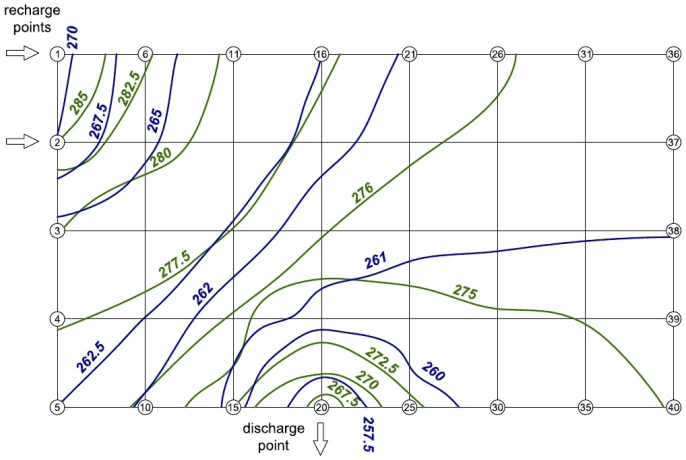

Fig. 4. Model case E. Green/brighter lines: laboratory model results, blue/darker lines: numerical model results. Labels show potential in cm.

with the laboratory analog results. A good agreement can be seen on Fig. 3.

Prominently high differences between the two modelling methods can be observed in case E (Fig. 4). The equipotential lines are parallel but the hydraulic losses in the numerical model are lower than in the laboratory model.

Only in case I was shape difference between the two modelling method. This could be caused by a change of geometry made in the laboratory model which could not be modelled in CFP. In laboratory model thicker pipes with a 32 mm diameter were linked to the original pipe system. The two pipes were too close to each other to model them separately; an idealisation was needed to model the effect of the thicker pipes. Although two different methods were tried out – the two pipes were substituted with one pipe: first, with a diameter calculated from the summarised cross-sectional area and second, with the hydraulic diameter – none of them gave the expected results (see Fig. 5 about the first running). The results of both idealisation are shown in Table 1, the values from the second running are in brackets.

Based on the parallel equipotential lines and the moderated differences between the losses of two modelling methods in most model cases the numerical model is acceptable.

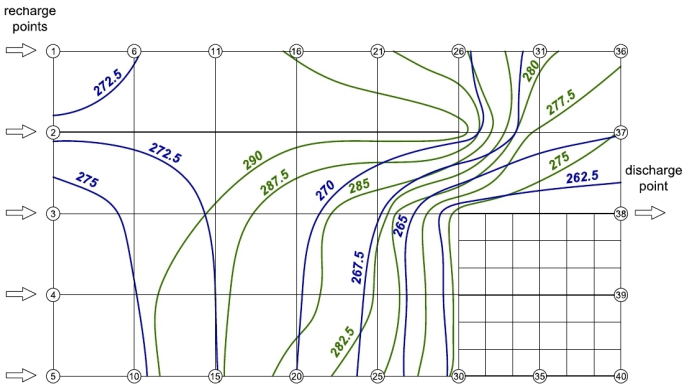

Fig. 5. Model case I. Green/brighter lines: laboratory model results, blue/darker lines: numerical model results. Labels show potential in cm.

2.4 Sensitivity analysis and additional usability

After the validation the effects of the calibrated parameters and the parameters assumed constant to the numerical results were analysed. The results of the sensitivity analysis are presented in Table 2.

According to the results it seems that the water temperature did not change the model results significantly. However, the choice for the upper and lower critical Reynolds-number can change the type of flow; in this case the original values led to better results but this sensitivity analysis of the Reynolds-

Tab. 2. Sensitivity analysis in laboratory model

Parameter	Initial value	New value	Change
Temperature	15°C	20°C	Lower hydraulic losses 0.5 - 1 cm
Reynolds-numbers	1000 / 2320	2320 / 4000	Turbulent flow became laminar Small hydraulic losses
Roughness	10^{-4} m	9×10^{-5} m	Errors +0.1 cm
		1.1×10^{-4} m	Errors - 0.4 cm, + 1 cm (D)
		10^{-3} m	No convergence
		10^{-5} m	Small hydraulic losses
Initial diameter	0.65 cm	0.6 cm	Errors + 20 cm (D)
		0.7 cm	Errors + 5 - 10 cm (C)

numbers showed the importance of the careful definition of these values.

The minor changes in the roughness caused minor differences from the original results and it became clear that only the order of magnitude of the roughness value is important. Contrarily the numerical results are very sensitive to the initial diameter: as long as the results of case C were improved with the 0.6 cm initial diameter the results of case D went wrong and vice versa with the 0.7 cm diameter. According to these results the originally used parameters are acceptable.

After the parameter sensitivity analysis the influence of the fix hydraulic head boundary condition on the model results was examined. The length of the model was duplicated. In the first case the length of the pipes was increased, in the second case the number of nodes was duplicated. The discharge data was from case A. Originally, the effect of the discharge could be detected in surrounding of the discharge point along about 0.6 m. When the length of pipes was duplicated the discharge affected zone did not change and in case of doubling of nodes this zone was 0.7 m. These results showed that the closeness of boundary conditions of the model did not disturb the flow pattern so the used length of the laboratory model is suitable to examine the effect of different discharge points and rates.

2.5 Summary of results of the laboratory model

The presented laboratory and numerical models are suitable models to examine the water flow in fractured rocks in which the permeability of primary porosity is negligible. These are able to model the effect of different discharge points and rates to the flow pattern and demonstrate the discharge affected zones. Although the models are very idealistic they can help the research of fractured rocks: these are able to help the understanding of water flow, support the field investigations and show the effect of different pipe geometries.

3 Modelling of a karst cave system

3.1 The introduction of the modelled area

The Molnár János Cave is a part of the Buda Thermal Karst located in Budapest, Hungary. With its more than 7.5 km known conduit system under the Rózsadomb the Molnár János Cave is the largest underwater cave system in Hungary [39]. The

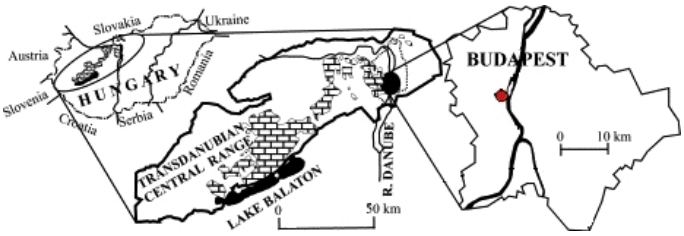

Fig. 6. Location of the Molnár János Cave (red dot). Modified from [45]

conduits are almost filled with lukewarm water; therefore cave divers have the main role in the investigation of the cave.

The Buda Thermal Karst is a part of the main karst aquifer of Transdanubian Range (see Fig. 6). Its sedimentary succession starts with carbonates from the Triassic Age (see Fig. 7). The most typical Triassic formation of the Rózsadomb area is the Main Dolomite (Hauptdolomit) Formation which is partly covered by Mátyáshegy Limestone Formation [40]. After the erosion of the Jurassic, Cretaceous and Palaeocene sediments shallow self carbonate layers were formed in Eocene Age [41]. The Szépvölgy Limestone Formation is the host rock of the extended cave system under the Rózsadomb (Pál-völgy Cave, Molnár János Cave, Mátyás-hegy Cave, Szemlő-hegy Cave, Ferenc-hegy Cave, József-hegy Cave) [40]. The limestone is overlaid by Buda Marl Formation, a partly calcareous marl which covers the greatest part of the Rózsadomb [40, 42]. Clay layers were formed in Oligocene Age; their physical parameters are quite similar to the older marl [40, 43]. Coastal sandstones and shallow marine limestone were formed in Oligocene-Miocene Age. The freshwater limestone from the Quaternary occurred in isolated patches at the area of the Rózsadomb [40, 41].

The only several tens of thousands year old Molnár János Cave was formed in the Eocene Age in the Szépvölgy Limestone and Buda Marl by "mixing corrosion" [39, 40, 45] (see Fig. 7). It means that waters with different temperature and ion content mix; this undersaturated water can dissolve the carbonate rocks along its secondary porosity. In this area the structurally-controlled mixing is the dominant cave forming process which has been still in progress [45]. The mixed water leaves the system through Alagút and Boltív Springs which feed Malom Lake, an artificial lake made in the 15^{th}-16^{th} centuries – first mentioned in 1540 – for the purpose of driving water mills [46]. A part of

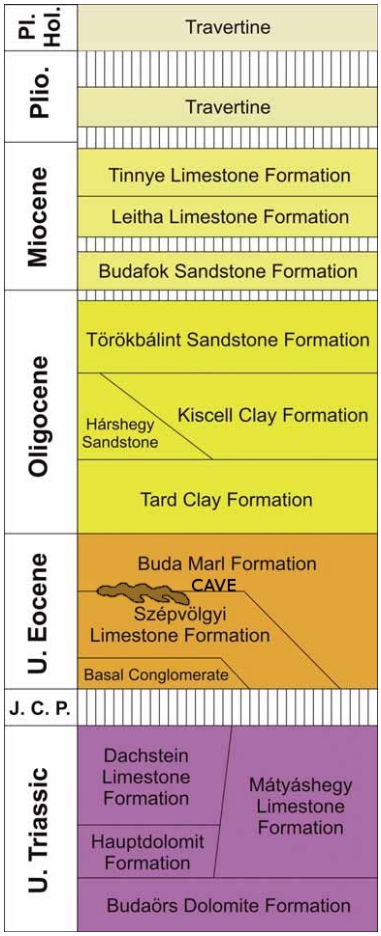

J Jurassic,
C Cretaceous,
P Paleocene,
Plio Pliocene,
Pl Pleistocene,
Hol Holocene.

Fig. 7. Litostratigraphic chart of the Buda Hills. Modified from [41]

the spring water is used by Lukács Thermal Bath; the other part flows in the lake and after flowing across a sluice it is led to the Danube. The cave system and its surroundings can be seen in Fig. 8.

The cave system is recharged by the water of intermediate and regional flow system [39]; previous studies detected that the cave water is not directly connected with local precipitation and probably only a slight amount of water comes from up local infiltration [47]. The water flow in the conduit system is not fully understood yet; only few measurement data are available about the discharge of springs and flow velocity in the cave. The main purpose of the presented modelling is try to better understand the flow system.

3.2 The model idealisations

As the first model made about the Molnár János Cave many idealisations and neglects were needed to build up a theoretically possible model. Only little information about the bedrock and the boundary conditions was available; the main and almost

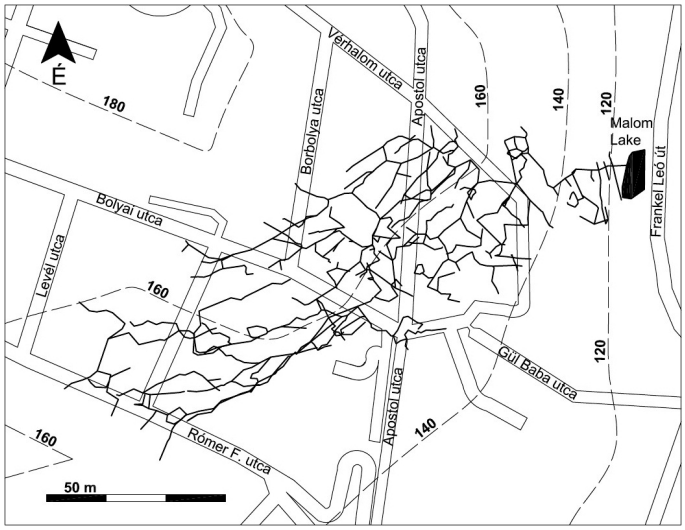

Fig. 8. The ground plane of the Molnár János Cave and its surroundings. Altitude isoline of terrain in m.a.s.l.

the only data was the known geometry of the cave system. Because of the filled conduits only the cave divers with simple tools could map the system. Therefore, the available geometry is a polyline, which approximately describes the rope system, which the divers installed in known conduits. The cross-sectional data used for the model was estimated by divers.

The investigation of the bedrock of the cave has recently started [48]; it is not properly known where the boundary of the different layers is. To simplify the model and according to the rock mechanical investigation it can be assumed that the most conduits are imbedded in the Szépvölgy Limestone. The hydraulic conductivity of the bedrock was not known; it was estimated with the help of the technical literature. The recharge of the area is ensured by unknown base flow; it could come from the rock matrix or along unknown fractures and conduits which lead water into the cave system. The only known discharge is the total discharge of the two springs at the Malom Lake; these could be handled as one spring because of their closeness to each other and because the available discharge data contains discharges of both

springs. It should be noted that unknown amount of water is led to the Lukács Thermal Bath. It is known that the water production of the Bath is not permanent but neither its amount nor the timescale of production is known. Conveniently this amount of water was neglected.

The modelling area was defined by the boundaries of the area being parallel and perpendicular to the main direction of the cave conduits. This means that the main flow direction is parallel to the longer boundaries (northwest and southeast) – it can be assumed that these are no-flow boundaries – and the shorter boundaries (northeast and southwest) could be defined as a constant head boundary.

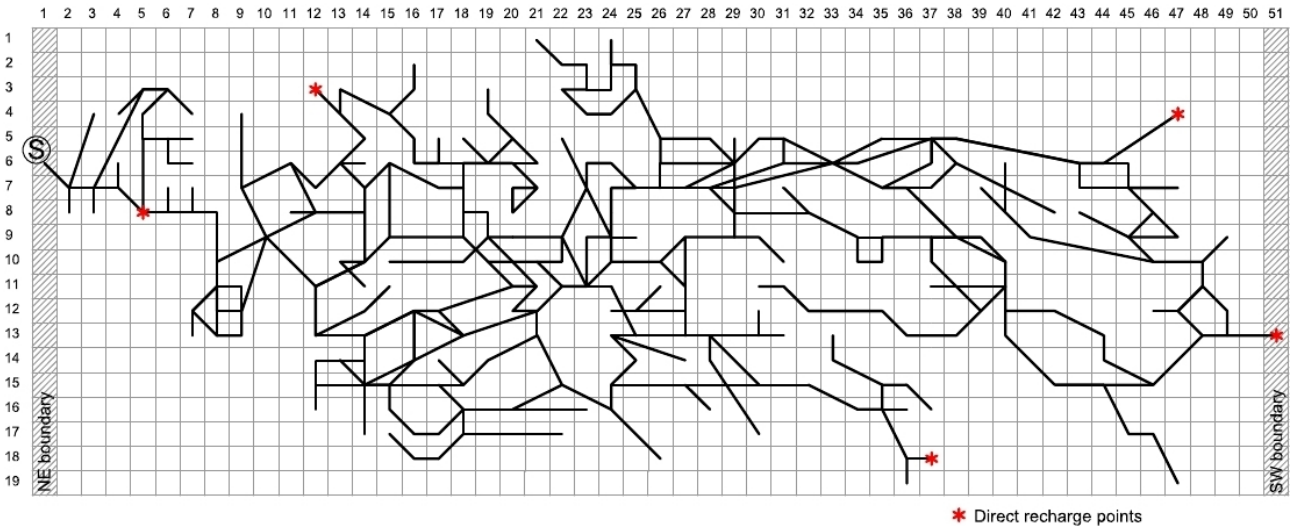

Fig. 9. The CFP model of the cave system (model size 190 x 510 m, grid cell size 10 m)

3.3 The numerical model

The numerical model of the cave was built in MODFLOW CFPv2 using Mode 1. Taking into account the accuracy of geometry data the cells have 10 x 10 m sizes. 19 rows, 51 columns and 10 layers were defined; the model domain has the overall dimension of 190 x 510 m (see Fig. 9). Most of the layers were 10 m thick, only the uppermost layer has variable thickness according to the topographical conditions. 316 nodes were imbedded into the centres of the cells; the cave conduits were modelled with circular pipes among nodes. 364 pipes were used with different diameters: the hydraulic diameter of the estimated cross-section. These cross sections were determined according to the field surveys of the cave divers. The conduit system was simplified into sections with uniform diameters: 28 different diameters were used from 0.89 m to 13.33 m. Although the laboratory scale model showed that the using of the hydraulic diameter does not lead to the perfect results especially in case of cross-sections, which shape is very different from a circle, it was the simplest and fastest method to generate circular pipes and taking into account the uncertainty of cross-sectional data. It should be an acceptable idealisation until more accurate measurement data would be available.

Because neither the exact location of layers nor their hydraulic parameters are known, each model layer was defined as one confined aquifer. The parameters of the limestone might have an important role in the flow and the rock mechanical results also showed that a significant part of the cave conduits are located in the Szépvölgy Limestone [48]; that is why the hydraulic properties of the rock layer were defined as limestone. Originally, the rock permeability was assumed to be 10^{-8} m/s both vertically and horizontally; this value is orders of magnitude higher than the hydraulic conductivity of a karstified, fractured limestone (10^{-2} - 10^{-4} m/s, for example: [1, 5, 12]) because the effect of karst conduits are taken into account with pipes. The mean height of the micro-topography of the pipe wall was defined as 0.01 m.

The purpose of the numerical modelling could not be to create a quite accurate model about the cave system and its area because of the many uncertainties; regular hydraulic and rock mechanical measurements just started in the recent past so very limited numbers of data are available. Therefore the modelling was focused on the following questions: how can water flow in conduits, what could be the role of the rock matrix and the exchange coefficient? Only discharge data of the outflow from the Malom Lake and some flow velocities in conduits are available [47, 49]. These data were checked in every model cases: the discharge rate is approximately 5 - 8 x 10^{-2} m^3/s and the maximum flow velocity is about 10^{-2} m/s although previous measurements provided different values [47]. The discharge was established with the help of a constant hydraulic head assumed to be 105 m.a.s.l. (where sea level is the Baltic Sea), which is approximately the lake water surface elevation - in the node “S” (spring, see Fig. 9.).

Three different model cases were analysed: the first, the “base flow” model where only the rock matrix recharged the cave conduits, the second, the “exchange” model where the effect of high exchange coefficient was analysed and the third, the “direct” model where the water in the conduits was ensured by direct water inflow at the end of the known conduits.

3.4 The base flow model case

In the base flow model the southwest boundary condition was defined as the ground level minus 10 m (between 140 and 150 m.a.s.l.), the northeast 105 m.a.s.l. was assigned. The water exchange coefficient was automatically calculated from the wall permeability by CFP. The original wall permeability was assumed to be 10^{-8} m/s – the same value as the hydraulic conductivity. These two parameters were decreased step by step until we reached the desired order of magnitude of the discharge rate and the flow velocity.

27 different cases were analysed in which the hydraulic conductivity and the wall permeability varied between 10^{-8} m/s

Tab. 3. Model cases in cave model

	Max. hydraulic head level ($m.a.s.l.$)	Hydraulic conductivity of the rock matrix (m/s)	Wall permeability (w, m/s) / exchange coefficient (e, m^2/s)	Discharge rate in the 1^{st} node (m^3/s)	Max. velocity in conduits (m/s)	Number of pipes with turbulent flow
Expected	-	-	-	5-8x 10^{-2}	10^{-2}	-
Base flow	150	10^{-6}	w: 10^{-6}	2×10^{-2}	2×10^{-2}	20
Exchange1	150	10^{-4}	e: 25	28.69	21.7	361
Exchange2	110	10^{-8}	e: 25	28.70	12.5	260
Direct	150	10^{-8}	w: 10^{-8}	3×10^{-2}	4×10^{-2}	21

and 10^{-4} m/s. The model was sensitive to both parameters. First the desired maximum velocity was reached where the hydraulic conductivity was 10^{-6} m/s and the wall permeability was 10^{-7} m/s. In this case the flow velocity was determined to 1.1×10^{-2} m/s and the spring discharge rate to 0.90×10^{-2} m/s, the flow became turbulent in few pipes. With increasing the hydraulic conductivity and/or the wall permeability the velocity and the discharge rate also increased. To reach the desired discharge rate the calculated velocity exceeded the estimated maximum velocity so a quite perfect matching could not be reach. As a general rule the orders of magnitude of velocity and discharge rate were acceptable where the hydraulic conductivity was between 10^{-6} and 10^{-5} m/s and the wall permeability was between 10^{-7} and 10^{-5} m/s. Where the hydraulic conductivity was more than hundred times or less than hundredths of the wall permeability the model led to wrong result: there were no flow pipes at the bottom of the model. A quite good result is presented in Table 3. In this case the flow became turbulent in eight percent of pipes.

3.5 The exchange model case

In MODFLOW CFP two options are available for assembling water exchange coefficient: the first, when the CFP calculates the exchange coefficient using pipe geometry data and the user-defined wall permeability data; the second, when the pipe conductance is entered by user in the CFP Input File. The first option was used in the base flow model where the wall permeability was estimated from the hydraulic conductivity of rock matrix. Although many existing studies suggest to set the conduit wall permeability to the order of hydraulic conductivity of the rock material encompassing pipes (for example: [50]); many authors showed that the results are very sensitive on the value of the wall permeability in this regime [50–52]. Chen et al. described a universal choice for the exchange coefficient: when this parameter is large (for example 25 m^2/s) the results is robust under perturbation on parameters and the relative error is small [53]. In this model case this universal value of the exchange coefficient was used.

Originally, the boundary conditions were the same as in the base flow model case – the maximum head level was 150 m.a.s.l. – and the hydraulic conductivity of the rock matrix was 10^{-6} m/s. The water exchange coefficient was defined to be 25 m^2/s. The flow became turbulent almost in every pipes and the discharge rate at the node one was 28.7 m^3/s. With decreasing the hydraulic conductivity of the rock matrix the flow velocity data and the discharge rate remained the same as in the first case. Many hydraulic conductivity values were tested from 10^{-12} m/s to 10^{-4} m/s but the results was the same in every case.

Then the constant hydraulic head level was decreased at the southwest boundary. The spring discharge rate remained 28.7 m^3/s even if the maximum level was only 110 m.a.s.l. However, the total volumetric exchange – flow between conduits and rock matrix – depended on the hydraulic head boundary condition: with decreasing the hydraulic head level the volumetric exchange also decreased. It meets the requirements because the volumetric exchange in a node is directly proportional to the hydraulic head difference between the head at the node and the head in the encompassing MODFLOW cell. In case of higher volumetric exchange (665.2 m^3/s from the matrix in the tubes) flow became turbulent in the most pipes - see Exchange case 1 in Table 3. Even at the lowest volumetric exchange (28.7 m^3/s from the matrix in the tubes) flow was turbulent in more than 70% of pipes – see Exchange case 2 in Table 3.

In this model case the desired discharge rate and maximum velocity value were not fulfilled but the results verify the statement of [53]: with wide range of the hydraulic conductivities the result was the same with use of a big exchange coefficient.

3.6 The direct model case

In this case four recharge points were defined at the end of the known conduits and one in the middle of the model (see Fig. 9). These points were those where the cave divers observed quite strong water flow or flow with different temperature. First, it was assumed that the direct recharge flow has the maximum velocity (0.01 m/s). The discharge rates calculated from this velocity were added to the node point as direct recharge. Both the wall permeability and the hydraulic conductivity of matrix were set to 10^{-8} m/s to avoid that the rock matrix could ensure the water in every conduit.

As a result it can be seen that the recharge rates of 0.01 m/s induced too high discharge rate at the springs: it was 3.00 m^3/s. The maximum velocity was also exceeded therefore the recharge

Tab. 4. Sensitivity analysis in cave model

Modified parameter	Original value of parameter	Modified value of parameter	Discharge rate in the 1^{st} node (m^3/s)	Max. velocity in conduits (m/s)	Number of pipes with turbulent flow
-	-	-	1.58×10^{-2}	2.01×10^{-2}	20
Temperature	21°C	30°C	1.58×10^{-2}	2.01×10^{-2}	34
		15°C	1.58×10^{-2}	2.01×10^{-2}	19
Reynolds-numbers	2000/ 10000	10/ 1000	1.58×10^{-2}	2.01×10^{-2}	150
		1000/ 2000	1.58×10^{-2}	2.01×10^{-2}	65
		4000 / 10000	1.58×10^{-2}	2.01×10^{-2}	10
Roughness	0.01 m	0.1 m	1.58×10^{-2}	2.02×10^{-2}	23
		0.001 m	1.58×10^{-2}	2.02×10^{-2}	25

rates were decreased. At the discharge velocity of 10^{-4} m/s the order of magnitude of the spring discharge rate and the maximum velocity in conduits became suitable: 3×10^{-2} m^3/s and 4×10^{-4} m/s (see Table 3.).

In every tested version there was no flow in about 10% of pipes. It means that the assumed recharge points could not ensure water in every conduit. The required water could come from the rock matrix as it was demonstrated in the base flow model or from more recharge points. The most probably possibility is that case where both sources ensure the water recharge.

With decreasing the discharge rates the number of pipes with turbulent flow also decreased.

3.7 Sensitivity analysis

Although the model results have many uncertainties the sensitivity analysis of the constant parameters could be important. In the cave model – according to the laboratory model results – the effect of temperature, critical Reynolds-numbers and wall roughness was analysed.

The MODFLOW CFP uses only one water temperature to calculate water flow in the model. It is known that there are zones in the Molnár János Cave with different water temperature. The upper limit of water temperature is about 30°C the lower limit is 15°C. These temperature data were tried out with the base flow model case where the wall permeability and hydraulic conductivity were 10^{-6} m/s. Neither the spring discharge rate nor the maximum velocity changed significantly with both temperatures. The water budget of the pipe system was the same in the original and modified models. The flow velocities in pipes changed not significant but this changing did not mean clear increase or decrease and it was under 10%. Only the number of pipes with turbulent flow changed: in the colder model case it was 19, in the hotter one it was 34 (see Table 4). These results showed that if the water temperature was in the feasible range, it did not change the model results significantly.

The analysis of the effect of the critical Reynolds-numbers led to the same results in the base flow model case. Only the numbers of pipes with turbulent flow was changed.

The effect of different Reynolds-numbers was also analysed in the exchange model case because in this case the number of the pipes with turbulent flow was much higher than in the base flow model case. The used modified Reynolds-numbers were the same as those in the base flow model case. However, the results were not sensitive to the change of the critical Reynolds-number. Neither the spring discharge nor the maximum velocity varied and the water budgets were the same. The number of pipes with turbulent flow did not change except where the critical Reynolds-numbers were 10 and 1000; in this case the flow became turbulent in every pipes. Because of this correspondence the results were not entered in the table to avoid redundancy. According to these trial cases it seems that the critical Reynolds-numbers do not play an important role in the results.

The order of magnitude change in wall roughness also did not vary the water budget and flow velocities. For details see Table 4.

3.8 Summary of results of the cave model

The presented numerical model about the Molnár János Cave is a suitable model to better understand flow in karst conduits. The model helped to investigate the source of recharge and the feasible role of rock matrix in flow. It seems that the exchange coefficient corresponds to the hydraulic conductivity of the rock matrix and the recharge can origin from the fractured and permeable rock matrix and also from unknown fractures and conduits connected to the known cave. The completed model is also able to be improved with new data from the ongoing cave research. In spite of many required idealisations the model results were very promising. The results can be used by divers and researchers to assign the pathway of the further investigation.

4 Conclusions

In this study a laboratory model and numerical models were presented. The quite good matching between the original laboratory model and its numerical model pointed out the usability and validity of both methods. The presented models are able to examine water flow in fractured rocks with low permeability of matrix. It showed that next to the often used numerical models also the old-fashioned laboratory models can help in the research of flow in fractured rocks and karst aquifers.

The first numerical model about the Molnár János was able to answer some carefully worded questions and contributed to the understanding of flow phenomena in cave system. The water in

conduits could origin from the primary porosity of the limestone surrounding the cave but also direct recharge points at the end of the known system could exist. It was showed that the exchange coefficient is a crucial parameter of the modelling. During the sensitivity analysis it became clear that against the results of the laboratory scale model the cave model is not very sensitive to the critical Reynolds-numbers and the roughness. The feasible water temperatures affected none of the models significantly.

The purpose of the different sensitivity for Reynolds-numbers and roughness could be origin from the flow velocities. In the laboratory scale model the sizes were small but the high velocities (about 2 m/s in the horizontal pipes in case A) caused turbulent flow with quite high hydraulic losses. In the cave model the turbulent flow was caused by the large cross-sectional area of the pipes and the velocities were small. Therefore, the hydraulic losses remained small because these are proportional to the flow velocity. The wall roughness also could not modify significantly the results because of these small velocities.

The analysis of hydraulic heads in nodes and trying new recharge points could be lead to important results. The presented models were steady-state models because of the limited data but later with long-time spring discharge data the transient modelling also could be possible. The diameters of pipes were the hydraulic diameter of the cross-sectional areas; may this method substitute with a better one.

The cave model can be improved by new research data to reach as proper model as it possible. That could lead a well usable model to analyse different influences to the cave system and it could help to better preserve this cave and also to better understand fractured and karst aquifers generally.

Acknowledgement

Special thanks to the cave diver group of Molnár János Cave, and Vilmos Vasvári and Zita Garamszegi to their kind help!

References

1 **Urbanc J, Mezga K, Zini L**, *An assessment of Capacty of Brestovica – Klarièi karst water supply (Slovenia)*, Acta Carsologica, **41**(1), (2012), 89–100, DOI 10.3986/ac.v41i1.50.

2 **Khaldi S, Ratajczak M, Gargala G, Fournier M, Berthe T, Favennec L, Dupont JP**, *Intensive exploitation of a karst aquifer leads to Cryptosporidium water supply contamination*, Water Research, **45**(9), (2011), 2906–2914, DOI 10.1016/j.watres.2011.03.010.

3 **Malard A, Vouillamoz J, Weber E, Jeannin P-Y**, *Swisskarst Project–toward a sustainable management of karst water in Switzerland. Application to the Bernese Jura*, In: Proceedings of the 13th National Congress of Speleology, Muotathal (SZ), Switzerland, 2012, pp. 215–219, http://neu.agsr.ch/wordpress/wp-content/uploads/215MalardetalSwisskarstProject.pdf.

4 **Downey JS**, *Geohydrology of the Madison and associated aquifers in parts of Montana, North Dakota, South Dakota, and Wyoming*, USGS, 1984, http://pubs.er.usgs.gov/publication/pp1273G.

5 **Bauer-Gottwein P, Gondwe BR, Charvet G, Marín LE, Rebolledo-Vieyra M, Merediz-Alonso G**, *Review: The Yucatán Peninsula karst aquifer, Mexico*, Hydrogeology Journal, **19**(3), (2011), 507–524, DOI 10.1007/s10040-010-0699-5.

6 **Tsang C F** (ed.), *Coupled processes associated with nuclear waste repositories*, Elsevier; London, 2012.

7 **Barenblatt G, Zheltov Y, Kochina I**, *Basic concepts in the theory of seepage of homogeneous liquids in fissured rocks*, Journal of Applied Mathematics and Mechanics, **24**, (1960), 852–864, DOI 10.1016/0021-8928(60)90107-6.

8 **Csoma R**, *Modelling the local variation of aquifer parameters with the help of the analytic element method*, Periodica Polytechnica Civil Engineering, **49**(2), (2006), 137–156, http://www.pp.bme.hu/ci/article/view/576/333.

9 **Copty NK, Trinchero P, Sanchez-Vila X**, *Inferring spatial distribution of the radially integrated transmissivity from pumping tests in heterogeneous confined aquifers*, Water Resources Research, **47**(5), (2011), DOI 10.1029/2010WR009877. this paper do not publish page numbers for some time past.

10 **Avci CB, Ufuk Sahin A**, *Assessing radial transmissivity variation in heterogeneous aquifers using analytical techniques*, Hydrological Processes, **28**(23), (2014), 5739–5754, DOI 10.1002/hyp.10064.

11 **Scanlon BR, Mace RE, Barrett ME, Smith B**, *Can we simulate regional groundwater flow in a karst system using equivalent porous media models? Case study, Barton Springs Edwards aquifer, USA*, Journal of Hydrology, **276**, (2003), 137–158, DOI 10.1016/S0022-1694(03)00064-7.

12 **Panagopoulos G**, *Application of MODFLOW for simulating groundwater flow in the Trifilia karst aquifer, Greece*, Environmental Earth Sciences, **67**(7), (2012), 1877–1889, DOI 10.1007/s12665-012-1630-2.

13 **Gargini A, De Nardo MT, Piccinini L, Segadelli S, Vincenzi V**, *Spring discharge and groundwater flow systems in sedimentary and ophiolitic hard rock aquifers: Experiences from Northern Apennines (Italy)*, In: **Sharp J M** (ed.), Fractured Rock Hydrogeology, CRC Press; Boca Raton, 2014, pp. 129–146, http://www.springer.com/de/book/9783642387388.

14 **Sauter M**, *Quantification and forecasting of regional groundwater flow and transport in a karst aquifer (Gallusquelle, Malm, SW. Germany)*, PhD thesis, Universität Tübingen, 1992, http://hdl.handle.net/10900/48838.

15 **Hao Y, Fu P, Carrigan CR**, *Application of a dual-continuum model for simulation of fluid flow and heat transfer in fractured geothermal reservoirs*, In: Proceedings, 38th Workshop On Geothermal Reservoir Engineering, vol SGP-TR-198., Stanford University; Stanford, California, 2013, pp. 462–469, http://pangea.stanford.edu/ERE/db/GeoConf/papers/SGW/2013/Hao.pdf.

16 **Borghi A, Renard P, Jenni S**, *A pseudo-genetic stochastic model to generate karstic networks*, Journal of hydrology, **414-415**, (2012), 516–529, DOI 10.1016/j.jhydrol.2011.11.032.

17 **Pardo-Igúzquiza E, Dowd PA, Xu C, Durán-Valsero JJ**, *Stochastic simulation of karst conduit networks*, Advances in Water Resources, **35**, (2012), 141–150, DOI 10.1016/j.advwatres.2011.09.014.

18 **Loper DE, Chicken E**, *A leaky-conduit model of transient flow in karstic aquifers*, Mathematical Geosciences, **43**(8), (2011), 995–1009, DOI 10.1007/s11004-011-9369-y.

19 **Hill ME, Stewart MT, Martin A**, *Evaluation of the MODFLOW-2005 Conduit Flow Process*, Groundwater, **48**(4), (2009), 549–559, DOI 10.1111/j.1745-6584.2009.00673.x.

20 **Gallegos JJ, Hu BX, Davis H**, *Simulating flow in karst aquifers at laboratory and sub-regional scales using MODFLOW-CFP*, Hydrogeology Journal, **21**(8), (2013), 1749–1760, DOI 10.1007/s10040-013-1046-4.

21 **Diersch H-J**, *FEFLOW. Finite Element Modeling of Flow and Heat Transport in Porous and Fractured Media*, Springer Science & Business Media, 2013, http://www.springer.com/de/book/9783642387388.

22 **Liedl R, Sauter M, Hückinghaus D, Clemens T, Teutsch G**, *Simulation of the development of karst aquifers using a coupled continuum pipe flow model*, Water Resources Research, **39**(3), (2003), DOI

10.1029/2001WR001206. this paper do not publish page numbers for some time past.

23 **Reimann T, Geyer T, Shoemaker WB, Liedl R, Sauter M**, *Effects of dynamically variable saturation and matrix-conduit coupling of flow in karst aquifers*, Water Resources Research, **47**(11), (2011), DOI 10.1029/2011WR010446. this paper do not publish page numbers for some time past.

24 **Rooij Rd, Perrochet P, Graham W**, *From rainfall to spring discharge: Coupling conduit flow, subsurface matrix flow and surface flow in karst systems using a discrete–continuum model*, Advances in Water Resources, **61**, (2013), 29–41, DOI 10.1016/j.advwatres.2013.08.009.

25 **Nordqvist AW, Tsang YW, Tsang C-F, Dverstorp B, Andersson J**, *Effects of high variance of fracture transmissivity on transport and sorption at different scales in a discrete model for fractured rocks*, Journal of contaminant hydrology, **22**(1), (1996), 39–66, DOI 10.1016/0169-7722(95)00064-X.

26 **Juhász J**, *Hidrogeológia (Hydrogeology)*, Akadémiai Kiadó; Budapest, 2002. (in Hungarian).

27 **Long JCS, Gilmour P, Witherspoon PA**, *A Model for Steady Fluid Flow in Random Three-Dimensional Networks of Disc-Shaped Fractures*, Water Resources Research, **21**(8), (1985), 1105–1115, DOI 10.1029/WR021i008p01105.

28 **Andersson J, Dverstorp B**, *Conditional simulations of fluid flow in three-dimensional networks of discrete fractures*, Water Resources Research, **23**(10), (1987), 1876–1886, DOI 10.1029/WR023i010p01876.

29 **Neretnieks I, Eriksen T, Tähtinen P**, *Tracer movement in a single fissure in granitic rock: Some experimental results and their interpretation*, Water Resources Research, **18**(4), (1982), 849–858, DOI 10.1029/WR018i004p00849.

30 **Moreno L, Neretnieks I**, *Flow and nuclide transport in fractured media: The importance of the flow-wetted surface for radionuclide migration*, Journal of Contaminant Hydrology, **13**(1), (1993), 49–71, DOI 10.1016/0169-7722(93)90050-3.

31 **Bear J, Tsang CF, De Marsily G**, *Flow and contaminant transport in fractured rock*, Academic Press; San Diego, 2012.

32 **Moreno L, Tsang YW, Tsang C-F, Hale FV, Neretnieks I**, *Flow and tracer transport in a single fracture: A stochastic model and its relation to some field observations*, Water Resources Research, **24**(12), (1988), 2033–2048, DOI 10.1029/WR024i012p02033.

33 **Shoemaker WB, Kuniansky EL, Birk S, Bauer S, Swain E D**, *Documentation of a Conduit Flow Process (CFP) for MODFLOW-2005. Techniques and Methods. Book 6, A-24.*, US Geological Survey; Reston, VA., 2007, http://pubs.usgs.gov/tm/tm6a24/.

34 **Öllős G, Németh E**, *Szakvélemény a repedezett kõzetekben lejátszódó folyamatok kisminta vizsgálatáról. (Study of the physical modeling of the flow processes in fractured rock)*, Budapest University of Technology and Economics, Faculty of Civil Engineering; Budapest, 1960. (in Hungarian).

35 **Öllős G**, *A karsztrendszerben lejátszódó hidraulikai folyamatok. (An Investigation into Hydraulic Phenomena in Karstic Systems)*, Hidrológiai Közlöny, **44**(1), (1964), 21–28, http://apps.arcanum.hu/hidrologia/a111126.htm?v=pdf&a=pdfdata&id=HidrologiaiKozlony_1964&pg=0&lang=hun#pg=22&zoom=f&l=s. (in Hungarian).

36 **Faulkner J, Hu BX, Kish S, Hua F**, *Laboratory analog and numerical study of groundwater flow and solute transport in a karst aquifer with conduit and matrix domains*, Journal of Contaminant Hydrology, **110**(1-2), (2009), 34–44, DOI 10.1016/j.jconhyd.2009.08.004.

37 **Wu Y, Hunkeler D**, *Hyporheic exchange in a karst conduit and sediment system–A laboratory analog study*, Journal of Hydrology, **501**, (2013), 125–132, DOI 10.1016/j.jhydrol.2013.07.040.

38 **Karay G, Hajnal G**, *Modelling of Groundwater Flow in Fractured Rocks*, Procedia Environmental Sciences, **25**, (2015), 142–149, DOI 10.1016/j.proenv.2015.04.020.

39 **Leél-Õssy S, Bergman C, Bognár C**, *A budapesti Molnár János barlang termálvizének veszélyeztetettsége. (The contamination risk of thermal water of the Molnár János Cave in Budapest)*, A Miskolci Egyetem Közleménye, A sorozat, Bányászat, **81**, (2011), 91–102, http://www.matarka.hu/koz/ISSN_1417-5398/81k_2011/ISSN_1417-5398_81k_2011_091-102.pdf. (in Hungarian).

40 **Kleb B, Benkovics L, Gálos M, Kertész P, Kocsányi-Kopecskó K, Marek I, Török Á**, *Engineering geological survey of Rózsadomb area, Budapest, Hungary*, Periodica Polytechnica Civil Engineering, **37**(4), (1993), 261–303, http://www.pp.bme.hu/ci/article/download/3822/2927&hl=hu&sa=T&oi=gsb-ggp&ct=res&cd=0&ei=GIyRVr_PH4TlmAHq667wAw&scisig=AAGBfm2D5N7YhemHoq72WO79mHjt8xDP-w.

41 **Götz AE, Török Á, Sass I**, *Geothermal reservoir characteristics of Meso- and Cenozoic sedimentary rocks of Budapest (Hungary)*, Zeitschrift der Deutschen Gesellschaft für Geowissenschaften, **165**(3), (2014), 487–493, DOI 10.1127/1860-1804/2014/0069.

42 **Görög P**, *Characterization and mechanical properties of the Eocene Buda Marl*, Central European Geology, **50**(3), (2007), 241–258, DOI 10.1556/CEuGeol.50.2007.3.4.

43 **Görög P**, *Engineering geologic properties of the Oligocene Kiscell Clay*, Central European Geology, **50**(4), (2007), 313–329, DOI 10.1556/CEuGeol.50.2007.4.2.

44 **Szanyi G, Surányi G, Leél-Õssy S**, *Cave development and Quaternary uplift history in the Central Pannonian Basin derived from speleothem ages*, Quaternary Geochronology, **14**, (2012), 18–25, DOI 10.1016/j.quageo.2012.09.001.

45 **Erõss A, Mádl-Szõnyi J, Surbeck H, Horváth Á, Goldscheider N, Csoma AÉ**, *Radionuclides as natural tracers for the characterization of fluids in regional discharge areas, Buda Thermal Karst, Hungary*, Journal of Hydrology, **426**, (2012), 124–137, DOI 10.1016/j.jhydrol.2012.01.031.

46 **Alföldi L, Bélteky L, Böcker T, Horváth J, Kessler H, Korim K, Oravetz J, Szalontai G**, *Budapest hévizei. (Thermal waters of Budapest)*, Vízgazdálkodási Tudományos Kutató Intézet; Budapest, 1968. (in Hungarian).

47 **Farkas D, Hajnal G, Szieberth D, Rehák A**, *A Molnár János-barlang térségének hidrológiai vizsgálata. (Hydrological investigation of the area of the Molnár János Cave.)*, In: **Török Á, Görög P, Vásárhelyi B** (eds.), Mérnökgeológia-Kõzetmechanika 2015, Hantken Kiadó; Budapest, 2015, pp. 61–74, http://www.mernokgeologia.bme.hu/ocs/index.php/konferencia/MGEO2015/paper/view/222/213. (n Hungarian).

48 **Pekáry A, Görög P, Hajnal G**, *Molnár János-barlang kõzetkörnyezetének mérnökgeológiai vizsgálata. (Engineering geology investigation of rock of Molnár János-cave.)*, In: **Török Á, Görög P, Vásárhelyi B** (eds.), Mérnökgeológia-Kõzetmechanika 2015, Hantken Kiadó; Budapest, 2015, pp. 149–160, http://www.mernokgeologia.bme.hu/ocs/index.php/konferencia/MGEO2015/paper/view/230/221. (in Hungarian).

49 **Lakos P**, *A Molnár János-barlang térségének hidrológiai vizsgálata. (Hydrological investigation of the area of the Molnár János Cave.)*, BSc thesis, Budapest University of Technology and Economics, Faculty of Civil Engineering, 2015. (in Hungarian).

50 **Bauer S, Liedl R, Sauter M**, *Modeling of karst aquifer genesis: Influence of exchange flow*, Water Resources Research, **39**(10), (2003), DOI 10.1029/2003WR002218. this paper do not publish page numbers for some time past.

51 **Birk S, Liedl R, Sauter M, Teutsch G**, *Hydraulic boundary conditions as a controlling factor in karst genesis*, Water Resources Research, **39**(1), (2003), SBH 2-1–SBH 2-14, DOI 10.1029/2002WR001308.

52 **Liedl R, Sauter M, Hückinghaus D, Clemens T, Teutsch G**, *Simulation of the development of karst aquifers using a coupled continuum pipe flow model*, Water Resources Research, **39**(3), (2003), DOI 10.1029/2001WR001206. this paper do not publish page numbers for some time past.

53 **Chen N, Gunzburger M, Hu B, Wang X, Woodruff C**, *Calibrating the exchange coefficient in the modified coupled continuum pipe-flow model for flows in karst aquifers*, Journal of Hydrology, **414**, (2012), 294–301, DOI 10.1016/j.jhydrol.2011.11.001.